Impact of build location on dimensional accuracy of 316L parts using SLM

M.A. Daoud *, M. Hayani Mechkouri, Y. Chairi, K.B. Haouari, K. Reklaoui

Faculty of Sciences and Techniques, University Abdelmalek Essaâdi, Tangier, Morocco
* Corresponding e-mail address: mddaoudd@gmail.com
ORCID identifier: https://orcid.org/0000-0002-0171-6073 (M.A.D.);
https://orcid.org/0000-0003-2141-3202 (M.H.M.); https://orcid.org/0000-0001-9749-4569 (Y.C.);
https://orcid.org/0000-0003-3553-7046 (K.B.H.); https://orcid.org/0000-0003-3701-7255 (K.R.)

ABSTRACT

Purpose: The objective of this study is to comprehensively investigate the printability characteristics of a selective laser melting (SLM) system, which will be achieved through the development of a benchmark test part. In addition, the effect of the build location on the dimensional accuracy and precision of 316 L stainless steel parts produced by SLM was thoroughly evaluated.

Design/methodology/approach: The benchmark part was designed using Catia CAD software. Parts were printed using a professional SLM 3D printer and 316L stainless steel powder as a material.

Findings: The results showed that to achieve exceptional dimensional accuracy in SLM parts, it is important to select the build location carefully. They also highlighted the critical role of gas distribution control in improving the precision of layer-by-layer deposition. The thorough evaluation of dimensional deviations at different build locations showed that optimal results were consistently achieved at position F within the build cham-ber.

Research limitations/implications: Further studies could investigate other factors affecting dimensional variations and surface roughness and enhance the comprehension of the interactions between the process parameters and the building position on the build platform.

Originality/value: The paper outlines the creation and production of a benchmark model used to assess the maximum capacity of SLM systems in manufacturing parts with ultimate dimensional precision. The effects of build location on dimensional accuracy are also explored in the given study.

Keywords: Additive manufacturing, Selective laser melting, 316L, Benchmark artefact, Dimensional accuracy

Reference to this paper should be given in the following way:

M.A. Daoud, M. Hayani Mechkouri, Y. Chairi, K.B. Haouari, K. Reklaoui, Impact of build location on dimensional accuracy of 316L parts using SLM, Archives of Materials Science and Engineering 125/2 (2024) 75-85. DOI: https://doi.org/10.5604/01.3001.0054.4683

MATERIALS MANUFACTURING AND PROCESSING

RESEARCH PAPER
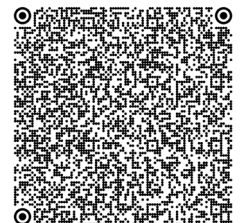
1. Introduction

Additive manufacturing (AM), also known as 3D printing, is a technology that produces objects by adding material in layers using data from a computer-aided 3D model, as opposed to traditional subtractive manufacturing processes [1]. Additive manufacturing (AM) has numerous benefits, such as the ability to fabricate intricate geometric shapes while minimising material waste, accommodating a broad range of part sizes and offering a variety of fabricating intricate geometric shapes while minimising material waste, accommodating a broad range of part sizes, and offering various material options [2]. Over the past few decades, additive manufacturing (AM) technology has experienced rapid expansion and found applications across various sectors, including medicine, automotive, aerospace, bioengineering, and other industries. Numerous processes have been devised, each grounded in distinct principles such as extrusion, melting, photopolymerisation, and sintering. The processes offer the advantage of working with an extensive array of highly precise materials, particularly for intricate geometries [3], and they enable enhanced design flexibility, frequently leading to the production of lightweight components [4].

Among the various metal additive manufacturing processes, Selective Laser Melting stands out as the most advanced powder bed fusion technique; it has gained widespread adoption, particularly in biomedical and aerospace applications [5]. SLM uses a high-power density laser to selectively melt and fuse metallic powders, producing near-net-shape parts with nearly full density (up to 99.9% relative density) [6,7].

Selective Laser Melting allows the fabrication of individual parts with intricate geometries that match the mechanical properties of components traditionally manufactured in large series. The process involves metallic materials such as steel, aluminium, titanium, and nickel-based alloys; the building is often filled with nitrogen or argon gas to establish an inert environment, preventing the hot metal pieces from undergoing oxidation.

Like other 3D printing techniques, the Selective Laser Melting (SLM) process comprises a sequence of phases, from slicing CAD data to removing printed pieces from the building plate [8].

Design guidelines are critical for increasing the efficiency and quality of parts manufactured using the SLM process. The guidelines have evolved in tandem with advances in manufacturing techniques, and they are now used as an effective tool for designers to choose a production method and generate optimal designs. Furthermore, design rules communicate new process capabilities to designers and engineers, allowing for a more in-depth exploration of the manufacturing process.

Many researchers have advocated using benchmarking parts, also known as "test artefacts," to improve precision and assess the capability of AM processes in consistently producing defect-free parts with intended dimensions [9]. Benchmark artefacts represent models for assessing the manufacturing process and machine performance. They can be customised to evaluate resolution, dimensional accuracy, repeatability, and surface roughness [10,11].

Moreover, establishing design rules tailored for various AM processes could enhance understanding of the technologies, providing users with new design freedoms [12].

The build location on the build platform can significantly impact the dimensional accuracy of SLM printed parts. Therefore, determining the best build location for SLM's build plate depends on various factors, including powder and gas flow distributions [13-16].

In the given paper, we present the design and fabrication of a Benchmark part to evaluate SLM system capacity in manufacturing different features with good surface quality. The goal here is to examine the geometrical performances of an SLM system by evaluating the dimensional accuracy of produced items in 316L stainless steel. Moreover, this study aims to investigate the impact of the build location on the build platform regarding the dimensional precision of complex geometries. By avoiding measurement constraints, the technology will produce a high-quality item that may even meet the existing tolerances of conventional machining.

2. Materials and methods

2.1. Design of benchmark part

Daniel Thomas was one of the first to develop design rules for metal additive manufacturing, especially specifically for the SLM process [17]. His work aimed to assess the SLM process and identify its geometric limitations.

The design of the benchmark test part followed the properties outlined by Byun et al. [18], complemented by adherence to existing ISO geometrical tolerance requirements [19-28].

It incorporates various sizes (small, medium, large) and forms of features such as holes, walls, cylinders, etc., arranged in all three axes. Our design procedure was initiated with a thorough analysis of the literature and a comparison of the most advanced test artefacts. Subsequently, selecting features in terms of type and size was based on insights from relevant studies and the established design rules. Finally, the test part was crafted based on these considerations.

The test part was created using CAD software, featuring 25 mm x 22.5 mm x 20 mm dimensions.

As illustrated in Figure 1, the test part comprises a variety of features, such as holes with diverse shapes (triangle, circle, square) and varying diameters (0.7 mm, 0.9 mm, 1.1 mm), three wall extrusions of varying dimensions (0.4 mm, 0.6 mm, 0.8 mm), successive wall cavities ranging from 0.2 mm to 1 mm, and three cylinders of different sizes (0.7 mm, 1 mm, 2 mm).

a)

b)

Fig. 1. a) CAD model of benchmark part, b) printed part

2.2. Material

The study used 316L stainless steel metal powder purchased from E-Plus-3D (Beijing, China) to produce the parts with SLM. Stainless steel is highly popular among various industries such as chemical, petrochemical, pharmaceutical, and home appliance [29].

To gain insight into the properties of the 316 L stainless steel powder, we employed Scanning Electron Microscopy (SEM) to examine its morphology and microstructure, which provided valuable information for various manufacturing applications. SEM analysis provided comprehensive insights into the characteristics of the metal powder. As

shown in Figure 2a, examination of the particle morphology revealed a predominantly spherical or irregular shape, consistent with the attributes commonly associated with metal powders produced through atomisation or equivalent methods. The assessment of the particle size distribution revealed a range extending from 25.8 μm to 61.8 μm.

a)

b)

Fig. 2. Microscopic insights into 316L stainless steel powder: a) Scanning Electron Microscopy (SEM) morphology images, b) energy-dispersive X-ray spectrum for chemical composition analysis

Table 1.
Chemical composition of 316L stainless steel

Composition, wt.%								
C	Mn	S	Si	Cr	Ni	Mo	N	O
<0.03	<2	<0.005	<1	16-19	9-13	1.5-3	<0.003	<0.002

Energy-dispersive X-ray Spectroscopy (EDS) was used to examine the chemical composition of the 316 L stainless-steel specimen. The examination was performed at an accelerating voltage of 15 kV and an acquisition duration of 60 s. The EDS spectrum, illustrated in Figure 2b, indicates the existence of several essential constituents in the 316 L stainless steel specimen. All those constituents are summarised in Table 1. The primary constituents confirmed were iron (Fe) and chromic (Cr), which agree with the alloy constitution. The weight percentages of Fe and Cr were determined to be approximately 68% and 17%, respectively. In addition to iron and chromium, trace amounts of other elements, including nickel (Ni), molybdenum (Mo), and manganese (Mn), were detected. Ni and Mo were present at approximately 12% and 2%, respectively, confirming the anticipated composition of 316 L stainless steel.

2.3. Printing and post-processing

Parts were printed using a SHINING 3D EP-M250 SLM 3D printer, equipped with a 500 W fibre laser, 70 µm spot size, 8m/s max scan speed, and 262 x 262 x 350 mm³ build volume. Argon gas was introduced into the SLM chamber to avoid oxidation of the samples while keeping the residual oxygen level below 1%.

The printing process employed specific parameters: a layer thickness configured at 50 µm, with the laser power set at 150 W and the scan speed at 700 mm/s.

After the SLM fabrication, the components underwent a thorough sandblasting procedure. The process involved projecting abrasive particles at high velocity onto the surfaces of the SLM parts. Sandblasting refines the exterior texture and removes residual powder particles, resulting in a smoother and cleaner final product. The further intervention significantly enhances the aesthetic appeal, surface finish, and functional properties of parts manufactured through SLM.

2.4. Experimental methodology

The experimental methodology used in the study comprised two distinct phases. In the initial phase, a benchmark component was printed to assess the ability of our Selective Laser Melting (SLM) system to reproduce all the specified characteristics and intricacies of the benchmark part. The second phase focuses on evaluating the influence of the building location of the part on the construction plate on the dimensional precision of the printed components. Accordingly, nine samples were fabricated on identical building platforms, each positioned at different locations denoted as A, B, C, D, E, F, G, H, and I, as illustrated in Figure 3. All samples were printed using the same set of process parameters as previously outlined.
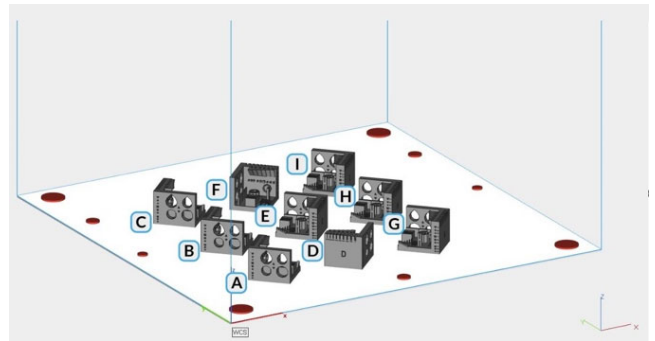

Fig. 3. Placement of samples on the building plate in 9 different positions

All features of the test part were measured employing a digital microscope, and all measurements were performed at least four times to obtain statistically significant results.

3. Results and discussion

3.1. Dimensional accuracy

Triangular holes

Figure 4a shows the printed triangular holes, which indicate that the prominence at the point of intersection between the two oblique geometric lines transforms from a pointed configuration to a rounded appearance. The observed phenomenon can be explained by considering the influence of the melt pool on the sharp region, leading to its transformation into a spherical shape.

Table 2 presents the measured dimensions of the triangular holes, and Figure 5a illustrates the average dimensional deviations from the designed dimensions. The average deviations indicate that the level of reproducibility

was within the acceptable range of dimensional error, with a maximum of 0.0433 mm for part E and a minimum of 0.0047 mm for part F.

Square holes

Figure 4b shows the printed square holes, indicating a significant alteration in their sharpness at the intersection of the two perpendicular line edges, from a pointed configuration to a rounded appearance, which can be explained by the same phenomenon observed for triangular holes. All nine samples' dimensions were measured and presented in Table 3. Figure 5b plots the average dimensional deviations from the nominal dimensions. The average deviation for all samples is within an acceptable accuracy range, with a minimum deviation of 0.0147 mm for sample F.

Circular holes

The printed circular orifices are illustrated in Figure 4c. All the measured dimensions of the tested components are listed in Table 4. A graph of the average dimensional deviations is displayed in Figure 5c. It highlights that the mean deviation for all samples falls within an acceptable range of precision, as sample F presents the smallest deviation of 0.0057 mm.

Walls

Wall extrusions

Figure 4d depicts the printed walls, and Table 5 provides the measurements for all the samples, along with the average dimensional deviations from their nominal dimensions. Walls measuring 0.6 mm thickness exhibit superior
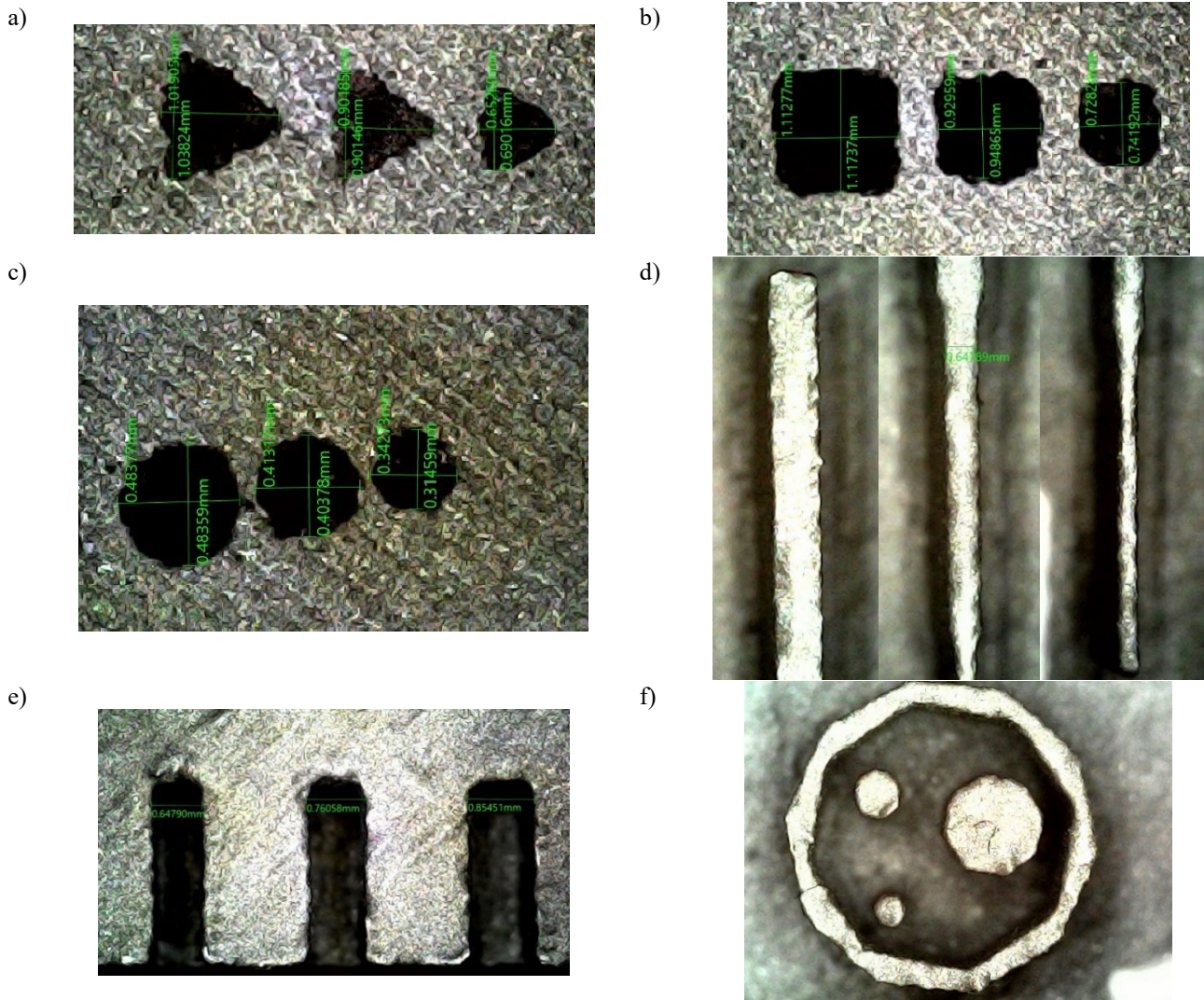
a)

b)

c)

d)

e)

f)

Fig. 4. Printed feature: a) triangular holes, b) square holes, c) circular holes, d) wall extrusions, e) Wall cavities, f) cylinders

dimensional accuracy with minimal deviation. Conversely, walls with thicknesses of 0.4 mm and 0.8 mm were printed at sizes below and above their nominal dimensions, respectively. This phenomenon can be attributed to the molten powder, which may accumulate owing to various factors, such as temperature fluctuations or inconsistencies in the printing process, causing a blockage in the recoater mechanism. As a result, the recoater fails to distribute the powder layer evenly, leading to uneven material deposition. The uneven deposition can adversely affect the quality and accuracy of the printed object, thereby preventing proper layer formation and causing defects in the final product.

The average dimensional deviations are depicted in Figure 5d, revealing that the mean deviation for all samples was within a satisfactory level of precision, with sample F exhibiting the least deviation of 0.0417 mm.

Wall cavities

The printed wall cavities are shown in Figure 4e. Measurements of all test parts are represented in Table 6, including the average of dimensional deviations from nominal dimensions. Walls with thicknesses ranging from 0.3 mm to 1 mm were printed with satisfactory dimensional accuracy. Nevertheless, walls with a thickness of 0.2 mm were not printed properly, displaying a substantial dimensional deviation of approximately 57% error, which can be explained by the same phenomenon discussed previously.

The graph displaying the mean dimensional deviations is presented in Figure 5e, demonstrating acceptable accuracy across all samples. Notably, Sample F had the least deviation, measuring 0.031 mm.
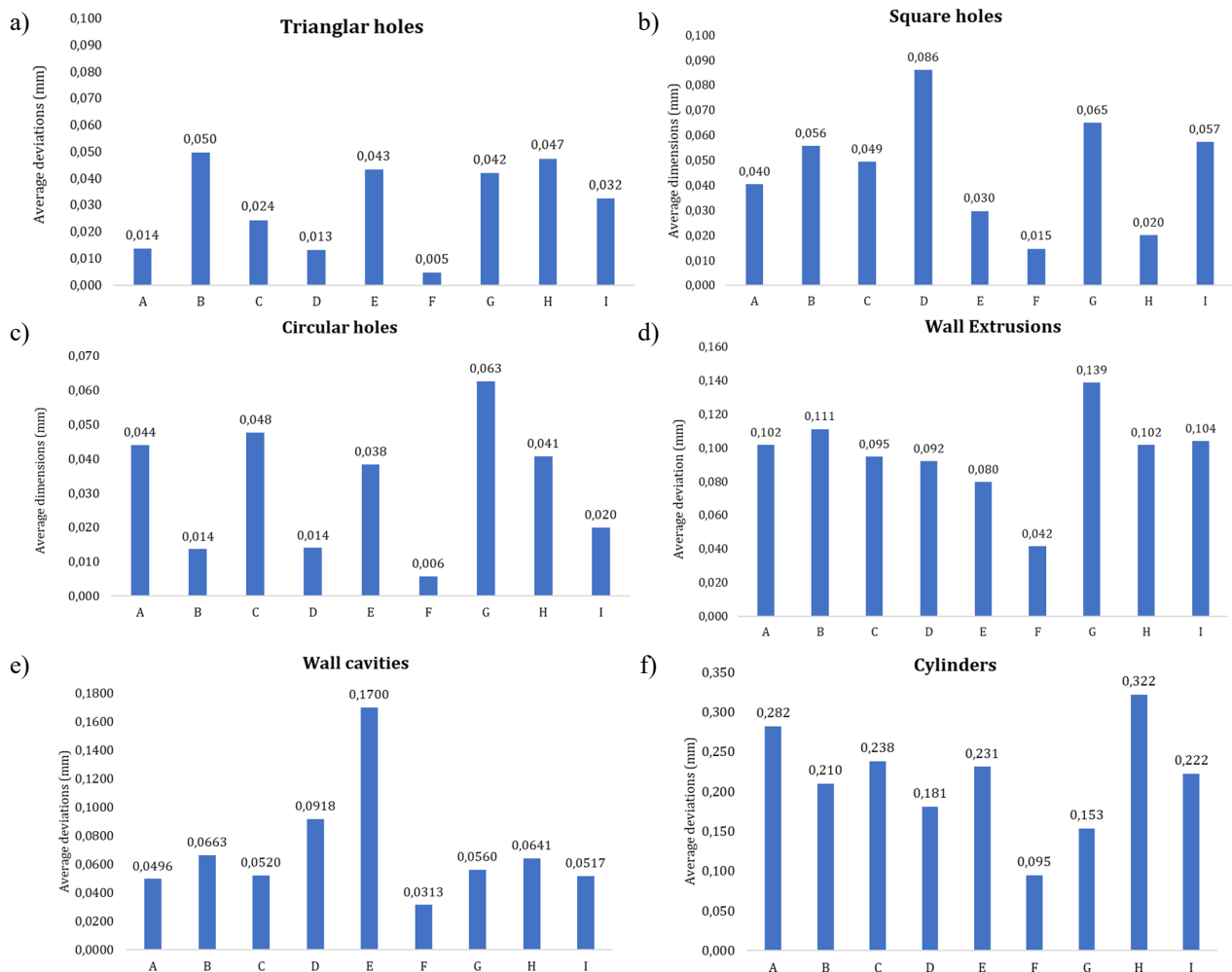

Fig. 5. Plot of the mean dimensional deviations: a) triangular holes, b) square holes, c) circular holes, d) wall extrusions, e) wall cavities, f) cylinders

Table 2.
Measurements of triangular holes

Features	Designed dimensions, mm	Measured dimensions, mm								
		A	B	C	D	E	F	G	H	I
Triangular holes	0.7	0.709	0.774	0.742	0.719	0.652	0.704	0.751	0.746	0.713
	0.9	0.915	0.944	0.929	0.883	0.901	0.908	0.967	0.863	0.962
	1.1	1.117	1.131	1.098	1.103	1.019	1.102	1.108	1.159	1.122
Average deviations		0.0137	0.0497	0.0243	0.0130	0.0433	0.0047	0.0420	0.0473	0.0323

Table 3.
Measurements of square holes

Features	Designed dimensions, mm	Measured dimensions, mm								
		A	B	C	D	E	F	G	H	I
Square holes	0.7	0.765	0.774	0.788	0.798	0.728	0.707	0.788	0.751	0.784
	0.9	0.92	0.971	0.943	0.996	0.944	0.927	0.976	0.906	0.943
	1.1	1.136	1.122	1.117	1.164	1.117	1.11	1.131	1.103	1.145
Average deviations		0.0403	0.0557	0.0493	0.0860	0.0297	0.0147	0.0650	0.0200	0.0573

Table 4.
Measurements for circular holes

Features	Designed dimensions, mm	Measured dimensions, mm								
		A	B	C	D	E	F	G	H	I
Circular holes	0.7	0.686	0.723	0.68	0.708	0.694	0.708	0.784	0.723	0.708
	0.9	0.868	0.915	0.854	0.877	0.877	0.896	0.845	0.84	0.873
	1.1	1.014	1.103	1.023	1.089	1.014	1.095	1.051	1.061	1.075
Average deviations		0.0440	0.0137	0.0477	0.0140	0.0383	0.0057	0.0627	0.0407	0.0200

Table 5.
Measurements of wall extrusions

Features	Designed dimensions, mm	Measured dimensions, mm								
		A	B	C	D	E	F	G	H	I
Wall extrusions	0.4	0.356	0.31	0.272	0.301	0.319	0.386	0.122	0.328	0.403
	0.6	0.685	0.676	0.573	0.638	0.61	0.61	0.572	0.704	0.676
	0.8	0.976	0.967	0.929	0.939	0.9483	0.901	0.91	0.929	1.033
Average deviations		0.1017	0.1110	0.0947	0.0920	0.0798	0.0417	0.1387	0.1017	0.1040

Cylinders

Figure 4f displays the printed cylinders, showing that the smaller cylinder was printed in an elliptical shape, in addition to a total distortion for sample H. The deformity can be due to uneven heat distribution during the printing process or rapid cooling, resulting in thermal distortions leading to the cylindrical shape taking on an elliptical form.

Table 7 provides a comprehensive overview of the measurements for all samples, and Figure 5f illustrates the mean dimensional deviation plot for each sample. Notably, the mean dimensional deviations fell within an acceptable range, from 0.321 mm for sample H to 0.0947 mm for sample F.

Table 6.
Measurements of wall cavities

Features	Designed dimensions, mm	Measured dimensions, mm								
		A	B	C	D	E	F	G	H	I
Wall cavities	1	1.037	1.065	1.032	1.028	1.037	1.01	1.056	1.037	1.014
	0.9	0.906	0.906	0.92	0.943	1.934	0.92	0.91	0.943	0.906
	0.8	0.831	0.849	0.821	0.863	0.854	0.802	0.845	0.849	0.845
	0.7	0.751	0.765	0.718	0.802	0.76	0.73	0.727	0.732	0.741
	0.6	0.643	0.662	0.647	0.709	0.647	0.611	0.671	0.685	0.638
	0.5	0.539	0.586	0.558	0.657	0.549	0.521	0.553	0.568	0.544
	0.4	0.469	0.474	0.483	0.474	0.464	0.458	0.469	0.488	0.469
	0.3	0.361	0.375	0.38	0.408	0.38	0.329	0.352	0.366	0.394
	0.2	0.309	0.315	0.309	0.342	0.305	0.301	0.321	0.309	0.314
Average deviations		0.0496	0.0663	0.052	0.0918	0.017	0.0313	0.056	0.0641	0.0517

Table 7.
Measurements of cylinders

Features	Designed dimensions, mm	Measured dimensions, mm								
		A	B	C	D	E	F	G	H	I
Cylinders	0.7	0.77	0.676	0.676	0.713	0.713	0.704	0.629	-	0.61
	1	1.24	1.117	1.136	1.098	1.145	1.02	1.061	1.117	1.051
	2	2.535	2.488	2.554	2.432	2.535	2.26	2.328	2.526	2.525
Average deviations		0.2817	0.2097	0.2380	0.1810	0.2310	0.0947	0.1533	0.3215	0.2220

3.2. The effect of build location on dimensional deviation

Extensive investigation is required to explore the influence of build location on the dimensional accuracy of Selective Laser Melting (SLM) components. This study aimed to uncover the impact of the spatial arrangement of components during the additive manufacturing process on the resulting dimensional discrepancies. The subsequent discussion presents an analysis of the obtained outcomes, emphasising the crucial insights gained into attaining optimal dimensional accuracy through prudent build location selection.

The results derived from the measurements of all nine test parts produced at different build positions showed a consistently acceptable range of dimensional deviation and, therefore, remarkable dimensional accuracy. Systematically exploring different build plate positions, each contributing to different thermal and environmental conditions during printing, provided reassuring results. It can be attributed to effective gas distribution management, as shown in Figure 6.
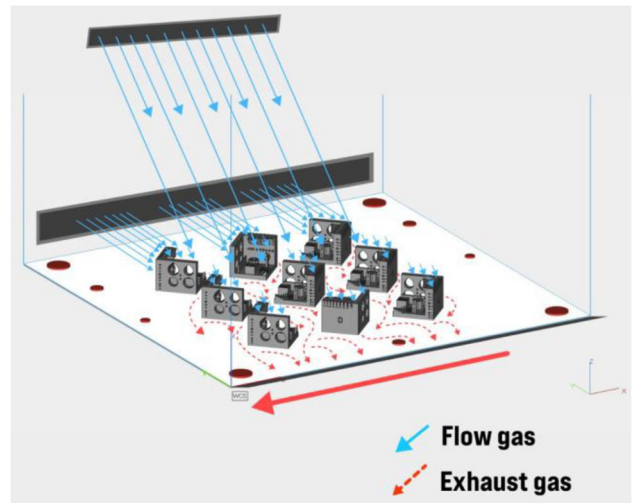

Fig. 6. Schematic of the distribution of gas flow within the build chamber

The figure illustrates the uniform gas distribution within the build chamber, which is crucial for temperature regulation,

minimising residual stresses, ensuring powder bed stability, and optimising the gas atmosphere. The implemented gas flow strategy improved layer-by-layer deposition precision by preventing overheating, promoting uniform cooling, and reducing hotspots.
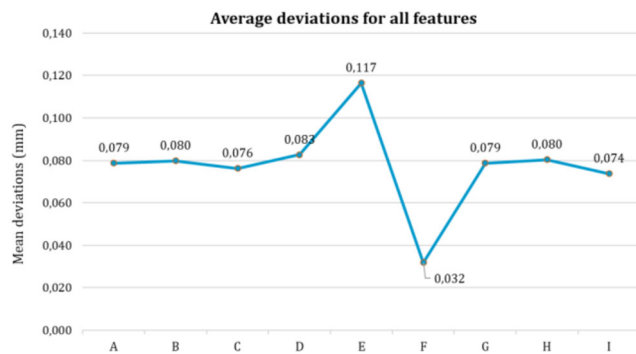

Fig. 7. Plot of mean deviations of all features for all samples

The mean deviations of all features for each sample across the nine build locations have been calculated and visually represented in Figure 7. Based on the graph, it is evident that location F within the building plate is the best option for our case and for achieving the maximum dimensional accuracy. We suggest that position F offers superior temperature control, which minimises thermal distortions and ensures the uniform solidification of metal powders. Moreover, a stable powder bed is maintained because of its location, which prevents agglomeration and encourages uniform layer deposition. The efficient gas flow dynamics at position F create an environment that minimises the powder's residual stresses, hotspots, and irregularities.

4. Conclusions

The study offers valuable insights into the dimensional accuracy of components produced using Selective Laser Melting (SLM) and how the location of the build affects the final product. A test part was developed to measure the dimensional precision of the manufactured components, focusing on aspects such as the walls, cylinders, openings, and hollow spaces.

The observed transformation in the geometrical shape of the sharp features, such as the shift from pointed to rounded configurations in triangular and square holes and variations in wall thickness, can be related to the impact of the melt pool. It highlights the significance of understanding the thermal dynamics and powder distribution during additive manufacturing.

The measured dimensions of printed features of all samples have shown an acceptable dimensional deviation compared to nominal dimensions. The effective gas flow distribution within the build chamber can explain this notable dimensional accuracy.

A comprehensive analysis of the mean deviations of all features for each sample across the nine build locations consistently identified position F within the build platform as the optimum location for achieving minimum dimensional deviations between the printed features and designed dimensions.

The research emphasises the important role of choosing the build location on the build plate to attain exceptional dimensional accuracy for Selective Laser Melting (SLM) parts. It underlines the crucial role of efficient gas distribution management in enhancing the accuracy of layer-by-layer deposition. Future investigations could further explore additional factors influencing the dimensional accuracy of SLM parts and improve understanding of the complex interplay between process parameters and build location.

References

[1] D. Zimmer, G. Adam, Direct Manufacturing Design Rules, in: P.J. Bártolo (ed), Innovative Developments in Virtual and Physical Prototyping, CRC Press, Boca Raton, 2011, 545-531.

[2] S. Bremen, W. Meiners, A. Diatlov, Selective Laser Melting: A Manufacturing Technology for the Future?, Laser Technik Journal 9/2 (2012) 33-38. DOI: https://doi.org/10.1002/latj.201290018

[3] H.-S. Byun, K.H. Lee, Design of a New Test Part for Bench-marking the Accuracy and Surface Finish of Rapid Prototyping Processes, in: V. Kumar, M.L. Gavrilova, C.J.K. Tan, P. L'Ecuyer (eds), Computational Science and Its Applications — ICCSA 2003, ICCSA 2003. Lecture Notes in Computer Science, vol. 2669, Springer, Berlin, Heidelberg, 2003, 731-740. DOI: https://doi.org/10.1007/3-540-44842-X_74

[4] L.A. Dobrzański, L.B. Dobrzański, A.D. Dobrzańska-Danikiewicz, Additive and Hybrid Technologies Forproducts Manufacturing Using Powdersof Metals, Their Alloys and Ceramics, Archives of Materials Science and Engineering 102/2 (2020) 59-85. DOI: https://doi.org/10.5604/01.3001.0014.1525

[5] F. Calignano, M. Lorusso, J. Pakkanen, F. Trevisan, E.P. Ambrosio, D. Manfredi, P. Fino, Investigation of Accuracy and Dimensional Limits of Part Produced in

Aluminum Alloy by Selective Laser Melting, The International Journal of Advanced Manufacturing Technology 88/1-4 (2017) 451-458.
DOI: https://doi.org/10.1007/s00170-016-8788-9

[6] W.S.W. Harun, K. Kadirgama, M. Samykano, D. Ramasamy, I. Ahmad, M. Moradi, Mechanical Behavior of Selective Laser Melting-Produced Metallic Biomaterials, in: J.P. Davim (ed), Mechanical Behaviour of Biomaterials, Woodhead Publishing Series in Biomaterials, Woodhead Publishing, Sawston, Cambridge, 2019, 101-116. DOI: https://doi.org/10.1016/B978-0-08-102174-3.00005-X

[7] G.D. Kim, Y.T. Oh, A Benchmark Study on Rapid Prototyping Processes and Machines: Quantitative Comparisons of Mechanical Properties, Accuracy, Rough-ness, Speed, and Material Cost, Proceedings of the Institution of Mechanical Engineers, Part B: Journal of Engineering Manufacture 222/2 (2008) 201-215.
DOI: https://doi.org/10.1243/09544054JEM724

[8] M. Seabra, J. Azevedo, A. Araújo, L. Reis, E. Pinto, N. Alves, R. Santos, J.P. Mortágua, Selective Laser Melting (SLM) and Topology Optimization for Lighter Aerospace Componentes, Procedia Structural Integrity 1 (2016) 289-296.
DOI: https://doi.org/10.1016/j.prostr.2016.02.039

[9] S. Moylan, J. Slotwinski, A. Cooke, K. Jurrens, M.A. Donmez, An Additive Manufacturing Test Artifact, Journal of Research of the National Institute of Standards and Technology 119 (2014) 429-459. DOI: https://doi.org/10.6028/jres.119.017

[10] L. Rebaioli, I. Fassi, A Review on Benchmark Artifacts for Evaluating the Geometrical Performance of Additive Manufacturing Processes, The International Journal of Advanced Manufacturing Technology 93/5-8 (2017) 2571-2598.
DOI: https://doi.org/10.1007/s00170-017-0570-0

[11] P. Subbaian Kaliamoorthy, R. Subbiah, J. Bensingh, A. Kader, S. Nayak, Benchmarking the Complex Geometric Profiles, Dimensional Accuracy and Surface Analysis of Printed Parts, Rapid Prototyping Journal 26/2 (2019) 319-329.
DOI: https://doi.org/10.1108/RPJ-01-2019-0024

[12] B.S. Rupal, R. Ahmad, A.J. Qureshi, Feature-Based Methodology for Design of Geometric Benchmark Test Artifacts for Additive Manufacturing Processes, Procedia CIRP 70 (2018) 84-89.
DOI: https://doi.org/10.1016/j.procir.2018.02.012

[13] M. Bayat, A. Thanki, S. Mohanty, A. Witvrouw, S. Yang, J. Thorborg, N.S. Tiedje, J.H. Hattel, Keyhole-Induced Porosities in Laser-Based Powder Bed Fusion (L-PBF) of Ti6Al4V: High-Fidelity Modelling and Experimental Validation, Additive Manufacturing 30 (2019) 100835.
DOI: https://doi.org/10.1016/j.addma.2019.100835

[14] K.Z. Ghumman, S. Ali, E.U. Din, A. Mubashar, N.B. Khan, S.W. Ahmed, Experimental Investigation of Effect of Welding Parameters on Surface Roughness, Micro-Hardness and Tensile Strength of AISI 316L Stainless Steel Welded Joints Using 308L Filler Material by TIG Welding, Journal of Materials Research and Technology 21 (2022) 220-236. DOI: https://doi.org/10.1016/j.jmrt.2022.09.016

[15] S. Pal, N. Gubeljak, T. Bončina, R. Hudák, T. Toth, J. Zivcak, G. Lojen, N. Leben, I. Drstvenšek, The Effects of Locations on the Build Tray on the Quality of Specimens in Powder Bed Additive Manufacturing, The International Journal of Advanced Manufacturing Technology 112/3-4 (2021) 1159-1170.
DOI: https://doi.org/10.1007/s00170-020-06563-5

[16] J. Kozhuthala Veetil, M. Khorasani, A.H. Ghasemi, B. Rolfe, I. Vrooijink, K. Van Beurden, S. Moes, I. Gibson, Build Position-Based Dimensional Deviations of Laser Powder-Bed Fusion of Stainless Steel 316L, Precision Engineering 67 (2021) 58-68. DOI: https://doi.org/10.1016/j.precisioneng.2020.09.024

[17] D. Thomas, The Development of Design Rules for Selective Laser Melting, PhD Thesis, Cardiff Metropolitan University, Cardiff, 2009. DOI: https://doi.org/10.25401/cardiffmet.20974597.v1

[18] I. Yadroitsev, L. Thivillon, Ph. Bertrand, I. Smurov, Strategy of Manufacturing Components with Designed Internal Structure by Selective Laser Melting of Metallic Powder, Applied Surface Science 254/4 (2007) 980-983.
DOI: https://doi.org/10.1016/j.apsusc.2007.08.046

[19] ISO/ASTM DIS 52904:2019, Additive manufacturing. Process characteristics and performance. Practice for metal powder bed fusion process to meet critical applications, ISO, Geneva, 2019.

[20] ISO/ASTM 52911-1:2019, Additive manufacturing. Design Part 1: Laser-based powder bed fusion of metals, ISO, Geneva, 2019.

[21] ISO 12780-1:2011, Geometrical product specifications (GPS). Straightness Part 1: Vocabulary and parameters of straightness, ISO, Geneva, 2011.

[22] ISO 12780-2:2011, Geometrical product specifications (GPS). Straightness Part 2: Specification operators, ISO, Geneva, 2011.

[23] ISO 12781-1:2011, Geometrical product specifications (GPS). Flatness Part 1: Vocabulary and parameters of flatness, ISO, Geneva, 2011.

[24] ISO 12781-2:2011, Geometrical product specifications (GPS). Flatness Part 2: Specification operators, ISO, Geneva, 2011.

[25] ISO 12180-1:2011, Geometrical product specifications (GPS). Cylindricity Part 1: Vocabulary and parameters of cylindrical form, ISO, Geneva, 2011.

[26] ISO 12180-2:2011, Geometrical product specifications (GPS). Cylindricity Part 2: Specification operators, ISO, Geneva, 2011.

[27] ISO 12181-1:2011, Geometrical product specifications (GPS). Roundness Part 1: Vocabulary and parameters of roundness, ISO, Geneva, 2011.

[28] ISO 12181-2:2011, Geometrical product specifications (GPS). Roundness Part 2: Specification operators, ISO, Geneva, 2011.

[29] M. Król, J. Mazurkiewicz, S. Żołnierczyk, Optimization and analysis of porosity and roughness in selective laser melting 316L parts, Archives of Materials Science and Engineering 90/1 (2018) 5-15. DOI: https://doi.org/10.5604/01.3001.0012.0607